Launch Load Resistant Spacecraft Mechanism Bearings Made From NiTi Superelastic Intermetallic Materials

Christopher DellaCorte [*] and Lewis E. Moore III [**]

Abstract

Compared to conventional bearing materials (tool steel and ceramics); emerging Superelastic Intermetallic Materials (SIMs), such as 60NiTi, have significantly lower elastic modulus and enhanced strain capability. They are also immune to atmospheric corrosion (rusting). This offers the potential for increased resilience and superior ability to withstand static indentation load without damage. In this paper, the static load capacity of hardened 60NiTi 50 mm bore ball-bearing races are measured to correlate existing flat-plate indentation load capacity data to an actual bearing geometry through the Hertz stress relations. The results confirmed the validity of using the Hertz stress relations to model 60NiTi contacts; 60NiTi exhibits a static stress capability (~3.1 GPa) between that of 440C (2.4 GPa) and REX20 (3.8 GPa) tool steel. When the reduced modulus and extended strain capability are taken into account, 60NiTi is shown to withstand higher loads than other bearing materials. To quantify this effect, a notional space mechanism, a 5 kg mass reaction wheel, was modeled with respect to launch load capability when supported on standard (catalogue geometry) design 440C; 60NiTi and REX20 tool steel bearings. For this application, the use of REX20 bearings increased the static load capability of the mechanism by a factor of three while the use of 60NiTi bearings resulted in an order of magnitude improvement compared to the baseline 440C stainless steel bearings.

Keywords

Bearings, mechanical components, rolling element bearings

Introduction

Spacecraft experience violent (shaking) and sustained (acceleration) inertial forces during launch because of the unsteady combustion provided by rocket propulsion systems (Ref. 1). Though each different launch vehicle presents a different vibration signature to its cargo, the launch load environments share certain characteristics. The launch loads are made up of a fairly steady average acceleration load of 3 to 6 g's plus a dynamic load that varies from 3 g's to over 9 g's depending upon whether the rocket utilizes solid propellants, liquid propellants or a combination of the two. In addition, spacecraft mechanisms often must endure additional shock type loads during deployment where the sudden release of spring energy and the use of pyrotechnic charges are encountered.

Such high environmental loads can lead to structural damage and payload damage, especially for delicate hardware. In response to these challenges, the space launch community has developed detailed design guidelines and testing protocols to mitigate negative outcomes (Ref. 1). One approach is to add design margin to flight hardware so that the damage load threshold is well above expected launch loads. This tends to add weight and expense. Another approach is to provide isolation of sensitive mechanisms to shield them from the launch environment. Such isolation systems can themselves be heavy and costly. In most instances, a combination of both approaches is used. Clearly, the development of more intrinsically robust mechanisms offers a path to ameliorate this issue.

[*] NASA Glenn Research Center, Cleveland, OH
[**] NASA Marshall Space Flight Center, Huntsville, AL

Inside space mechanisms, the contacts between balls and races in ball bearings are a primary vulnerability for launch load damage. Spacecraft mechanisms rely on ball bearings for smooth and low friction operation of a wide array of systems such as deployment mechanisms, pointing gimbals and flywheels used in gyroscopes and reaction wheels. If a bearing raceway surface is dented by a static overload event, such as might occur during launch, the bearing may not run sufficiently smoothly and may fail prematurely (Ref. 2). Over the years, bearing and mechanism designers have developed at least four main strategies to overcome this problem.

One strategy is to devise mechanism locking features to divert loads around the bearings through other static structures thereby protecting precision bearing rolling surfaces. Another strategy is to carefully design and tailor internal bearing geometry to increase the load capacity of the ball-race contact. A third approach involves careful orientation of the mechanism with respect to the anticipated static load direction such that any damage that occurs is manifested outside the rolling contact zone. Finally, judicious material selection can be done leading to the use of race materials with heightened load capability. Unfortunately, each of these strategies carries inherent disadvantages.

Locking mechanisms can be complex to design, add weight and can fail to deploy correctly. This can lead to failure of the mechanism these devices are supposed to protect. Careful design of the bearing geometry, increasing conformity of the race-ball contact, can reduce stress levels but leads to increased operating friction. Further, such geometrical changes have only a marginal effect on load capability. The number and size of the bearing balls can be changed to maximize load capacity but this has the effect of increasing cage friction and reducing cage strength and lubricant reservoir capacity. Preferential orientation of a payload within the spacecraft can only alleviate predictable, directional launch loads such as vertical acceleration. Such an approach is ineffective for random vibrational loads. Finally, choosing higher strength materials such as substitution of high carbide tool steel for martensitic stainless steel has other tradeoffs like poor corrosion resistance (Ref. 3). Clearly there is a need for a fresh approach to enhance a bearing's ability to withstand static contact loads in spacecraft mechanisms. The use of superelastic intermetallic materials (SIMs) is such an approach.

Superelastic Intermetallic Materials like 60NiTi have been researched sporadically for over half a century but only recently have they been considered and matured for use in rolling element bearings (Refs. 4 and 5). Their use in highly loaded, high contact stress devices like bearings and gears initially appears counter intuitive. Traditional mechanical component materials like tool steel and silicon nitride have high hardness and elastic modulus and very limited elastic strain deformation range. These properties give components like bearings very high stiffness thus limiting deflection under load resulting in precise and predictable motion control, low friction and long life. Superelastic materials, like 60NiTi, exhibit material properties that differ significantly from those for traditional bearing materials.

The NiTi alloys have an elastic modulus (stiffness) that is less than half that for steel and one third that of ceramics like silicon nitride. Despite developing high hardness comparable to tool steel through heat treatment, the superelastics can endure very large strains (5 percent or more) in a fully elastic manner. This elastic range is an order of magnitude or more higher than steel and ceramic. The unique combination of properties (high hardness, relatively low modulus, high elastic strain range) results in high resistance to concentrated contact damage such as Brinell indentation denting.

In a series of earlier studies, hardened 60NiTi flat plate surfaces were dented with silicon nitride balls to determine its resistance to damage and to establish stress limits for bearing design guidance (Ref. 6). It was shown that increases in contact stress led to an increase in permanent dent depth. Further it was found that, on a stress basis, 60NiTi's capability fell between that of 440C stainless steel and the high carbide content REX20 tool steel. Figure 1 depicts the stress-dent depth behavior.

Figure 1. Dent Depth Versus Mean Contact Stress for 12.7 mm Diameter Si_3N_4 Ball Pressed Onto Flat Plate Specimens.

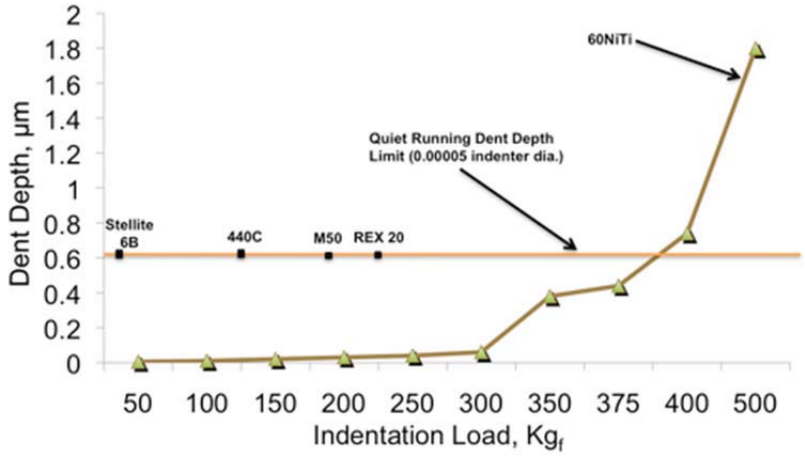

Figure 2. Dent Depth Versus Indentation Load for 12.7 mm Diameter Si_3N_4 Ball Pressed Onto Flat Plate Specimens.

When the same data is plotted on a load-dent depth basis, however, the rankings differ dramatically. The reduced modulus of elasticity for 60NiTi combined with its high elastic range enable very high loads prior to the formation of significant permanent dents. In fact, as shown in Figure 2, on the basis of applied load, 60NiTi can withstand 3 to 5 times higher loads than even the most advanced bearing steel.

The results shown in these two figures were then further extended to 60NiTi surfaces that were enhanced by pre-stressing. When pre-stressed by 2.70 GPa, the dent resistance increases by about 30 percent (Ref. 7). This stress capability increase translates into a 50 percent improvement in static load capacity. Figure 3 shows this data. Clearly, even at this nascent stage of technological development, the resilience of NiTi offers a potential path to very robust bearings and mechanisms.

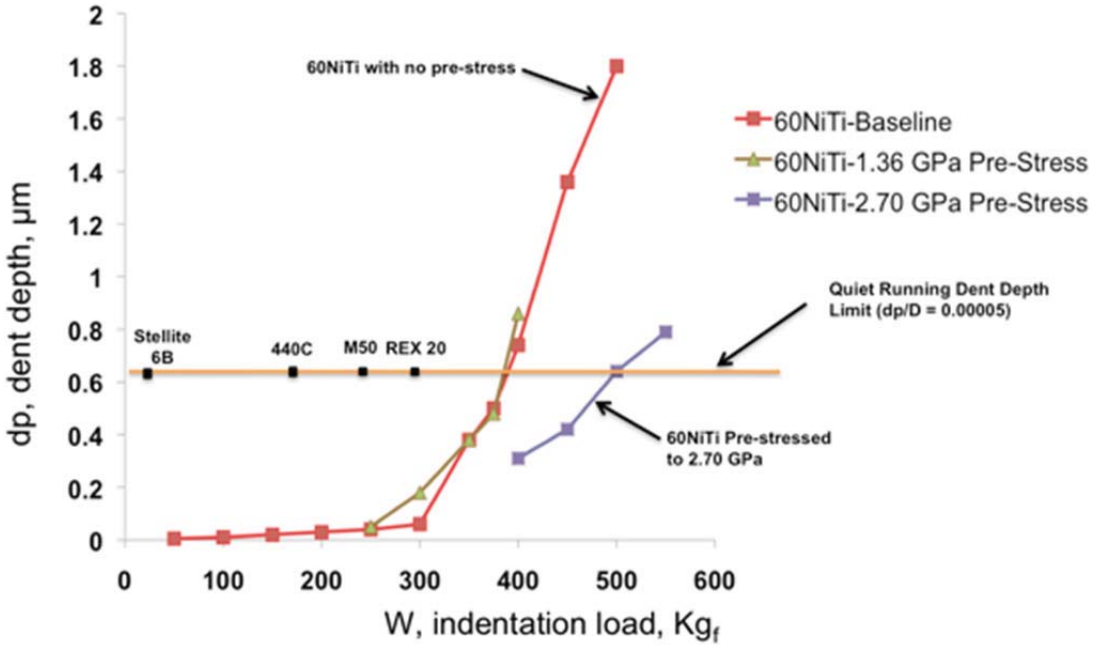

Figure 3. Dent Depth Versus Indentation Load for 12.7 mm Diameter Si_3N_4 Ball Pressed Onto Previously Stressed 60NiTi Flat Plate Specimens (Ref. 7).

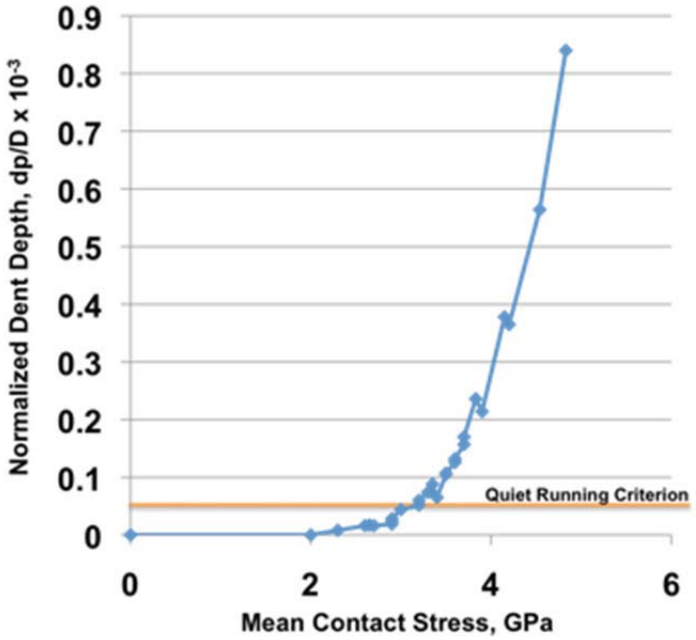

Figure 4. Normalized Dent Depth Versus Mean Hertz Contact Stress for Si_3N_4 Balls From 6.4 to 12.7 mm Diameter Pressed Onto 60NiTi Flat Plate Specimens.

However, all of these early results were limited to indenters of the same size, 12.7 mm diameter. For design purposes, the stress and load capacity of NiTi must be evaluated for a wide range of indenter sizes. These experiments were recently reported for silicon nitride indenter balls from 6.35 to 12.7 mm diameter (Ref. 8, to be published). When the Hertz equations were used to collate the dent depth data as a function of stress, the data for all ball sizes fall onto the same curve as shown in Figure 4.

Based upon these flat plate results, one can conclude that the Hertz stress model is useful in predicting denting behavior of NiTi. Further, the behavior of NiTi to static loads is the same whether the indentation is from a small ball or a large ball. In order to complete the assessment and establish a stress capability limit that can be used with confidence for bearing design, however, the dent capability of a real bearing race, with dual curvature must be measured.

In the present study, a series of experiments are carried out in which the inner race of a 50 mm ball bearing is loaded by a single 8.74 mm (0.344 in.) diameter silicon nitride ball under loads that range from 2200 to 11,000 N (1000 to 5000 lb). These loads correspond to mean Hertz contact stress from 2.1 to 3.5 GPa. The resulting dents are characterized for form, shape and depth. This data is then used to firmly establish load capability of 60NiTi bearing races. In addition, the newly established stress capability is then applied to the design of ball bearings that support a simple notional space mechanism, a reaction wheel. By analysis, the wheel assembly is then put through estimated space vehicle launch loads to determine its ability to survive without damage.

Materials and Procedures

The test specimens consist of a ceramic indenter ball and a 60NiTi bearing race. The indenter is a standard grade 5 Si_3N_4 bearing ball (8.74 mm dia.) and the inner race of a 50 mm bore ball bearing made from 60NiTi. The general material properties of these materials are shown alongside more conventional tool steel bearing materials in Table 1.

Table 1. Nominal Properties for 60NiTi and Si_3N_4 Test Specimens and Conventional Bearing Steels

Property	60NiTi	440C	Si_3N_4	M-50
Density	6.7 g/cc	7.7 g/cc	3.2 g/cc	8.0 g/cc
Hardness	56 to 62 HRC	58 to 62 HRC	1300 to 1500 Hv	60 to 65 HRC
Thermal conductivity W/m-°K	~9 to 14	24	33	~36
Thermal expansion	$\sim 11.2\times10^{-6}$/°C	10×10^{-6}/°C	2.6×10^{-6}/°C	$\sim 11\times10^{-6}$/°C
Magnetic	Non	Magnetic	Non	Magnetic
Corrosion resistance	Excellent (Aqueous and acidic)	Marginal	Excellent	Poor
Tensile/(Flexural strength)	~1000(1500) MPa	1900 MPa	(600 to 1200) MPa	2500 MPa
Young's Modulus	~95 GPa	200 GPa	310 GPa	210 GPa
Poisson's ratio	~0.34	0.3	0.27	0.30
Fracture toughness	~20 MPa/√m	22 MPa/√m	5 to 7 MPa/√m	20 to 23 MPa/√m
Maximum use temp	~400 °C	~400 °C	~1100 °C	~400 °C
Electrical resistivity	$\sim 1.04\times10^{-6}$ Ω-m	$\sim 0.60\times10^{-6}$ Ω-m	Insulator	$\sim 0.18\times10^{-6}$ Ω-m

Silicon Nitride is a hard ceramic material that is increasingly being used for balls in rolling element bearings because of its excellent corrosion resistance, low density and fatigue life capability. Under the poorly lubricated conditions, ceramic-steel hybrid bearing configurations are typically more wear resistant than all-steel bearings.

The bearing race is made from powder metallurgy processed 60NiTi manufactured according to the steps detailed previously in the literature (Ref. 9). Briefly, pre-alloyed powder is made by atomization using 60 wt% nickel and 40 wt% titanium feedstock. The powder is placed inside an evacuated mild steel can that is then sealed by welding. The canned powders are consolidated under high pressure and temperature resulting in a fully dense 60NiTi ingot. The ingot is cut using a combination of electric discharge machining, turning and grinding operations to produce slightly oversized bearing races. The races are then heat treat hardened, finish ground and polished to produce bearing quality races as shown in Figure 5.

Figure 5. 60NiTi Bearing Races.

In order to estimate the static load capacity (permanent dent resistance) of a 60NiTi hybrid bearing one first needs to measure the load limit of a single ball-race contact. When one ball contacts a race, the load limit is reached when the Hertz contact stress exceeds that necessary to create a permanent dent whose depth is approximately 0.00005 times that of the ball diameter. This dent depth magnitude corresponds to a damage threshold which when exceeded leads to rough bearing operation and potentially reduced fatigue life (Ref. 2). The Hertz equations are used to calculate the contact stress. The stress is a function of the load, the geometries and material properties of the ball and race. The bearing geometry evaluated adheres to conventional design norms. The ball has a radius of 4.37 mm and the race curvatures are nominally 4.55 and 27.4 mm in the cross race and ball path (circumferential) directions, respectively. This gives the bearing ball-race conformity a value of 52 percent, a value very typical for ball bearings (Ref. 10). Since the inner race-ball contact represents the most severe stress location in a ball bearing, it is selected in the present study as the location of interest.

A special fixture was designed and fabricated to firmly hold the inner race and present it to a single ceramic ball for loading experiments. Figure 6 shows the fixture that is made up of two V-blocks that cradle a solid steel shaft onto which the bearing race is mounted. The steel shaft is marked to aid in placing the indents and is easily rotated while the fixture is mounted in a standard materials test load frame.

To conduct a test, the race fixture is placed on the lower platen of the load frame and help in place with two C-clamps. The ball pushrod is placed in the hydraulically actuated grip of the upper platen. A small amount of silicone vacuum grease is placed into the hemispherical cavity machined into the lower end of the ball pushrod. The ceramic indenter ball is placed into the cavity and the grease prevents the ball from falling out during unloaded periods of testing. The load frame is computer controlled using the desired test load as the control parameter.

To run a test, the ball pushrod is lowered at low speed by the computer until contact with the race is detected. The test load is then gently applied over approximately a five second ramp-up period and then held for 60 s. The load is then removed and the race shaft is rotated to the next desired test location. Dent locations are spaced equally 12° apart around the circumference of the race. After the dent experiments are complete, the fixture is removed and placed into an optical surface profilometer for dent depth characterization.

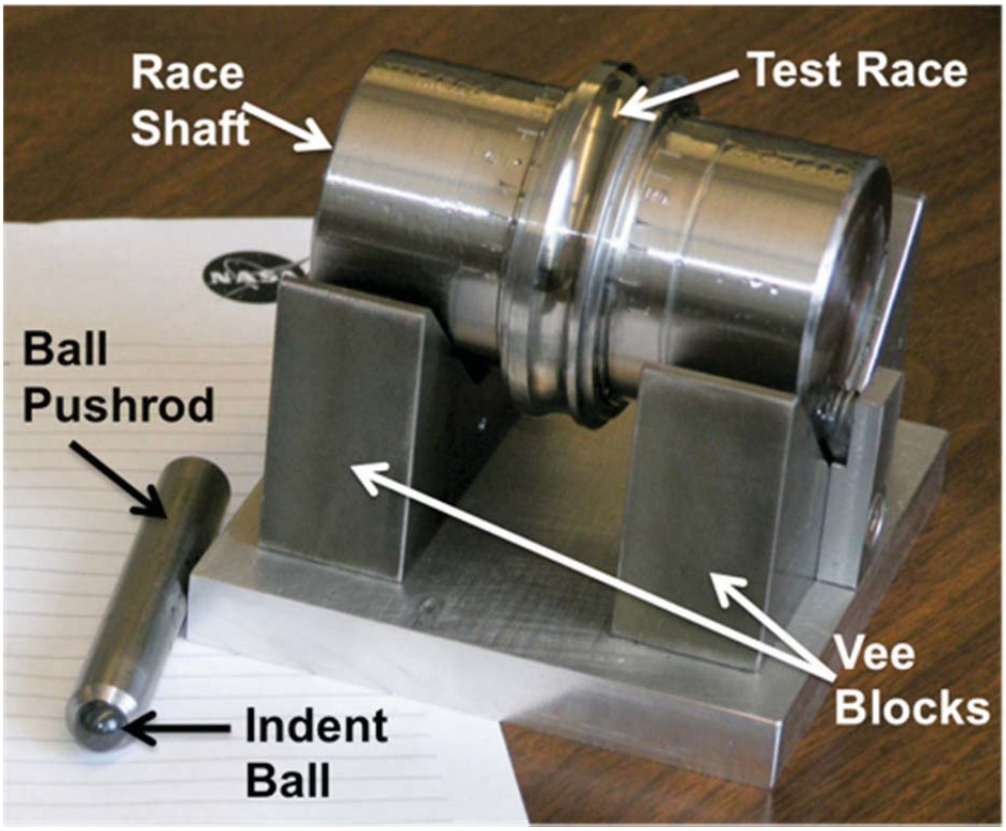

Figure 6. Bearing Race-Ball Dent Fixture.

Results and Discussions

The single ball versus race static load capacity of a hybrid Si_3N_4-60NiTi bearing was evaluated and the results are shown in Table 2. In the table, the dent depth, dent depth normalized by the ball diameter, the peak stress and the mean stress are listed. The normalized dent depth as a function of mean stress is plotted in Figure 7.

The dent depth data for the ball-race contact agrees reasonably well with the more generalized ball-flat plate dent depth data collected previously (Ref. 8). This agreement, despite differences in contact geometry, further support the argument that the Hertz stress relations for contacting bodies can be confidently applied to bearing design. Using the generally accepted dent depth criteria (dp/D~0.00003 to 0.00010), the data indicate that the damage threshold for 60NiTi is around 2.8 to 3.3 GPa. This is slightly lower than the value estimated from flat plate dent studies but within data scatter and is to be considered in good agreement. Further experiments with additional race sizes are warranted to narrow the stress limit more precisely. For the present, a reasonable stress limit, when designing bearings to withstand high static load, is 3.1 GPa.

In the section that follows, a notional spacecraft mechanism, a small reaction wheel assembly (RWA), will be assessed to determine how the substitution of 60NiTi for steel in the bearings can affect the ability to withstand the rigorous launch vibration load environment. Through such an assessment it is hoped that pathways to performance improvement, weight reduction or enhanced robustness will be revealed.

Table 2. Indentation Depth Data Summary

[{Si_3N_4 Ball (8.74 mm dia.) loaded against hardened (HRC 60.5) polished 60NiTi inner race} Inner Race Curvature Radii: ball-path, 4.25 mm; cross-race, 1.27 mm.]

Indent load, Kg_f (lb)	Mean stress, GPa (ksi)	Peak stress, GPa (ksi)	Dent depth,[a] μm (μin.)	Dent depth/Ball dia., $\times 10^{-4}$
493 (1000)	2.05 (298)	3.07 (446)	None detected	-----
741 (1500)	2.40 (348)	3.52 (511)	None detected	-----
988 (2000)	2.59 (375)	3.88 (562)	0.19 (7.5)	0.22
1111 (2250)	2.69 (390)	4.03 (585)	0.12 (4.8)	0.14
1235 (2500)	2.79 (404)	4.18 (606)	0.59 (23.3)	0.68
1358 (2750)	2.88 (417)	4.32 (626)	0.55 (21.8)	0.63
1482 (3000)	2.96 (429)	4.44 (644)	0.80 (31.4)	0.92
1605 (3250)	3.04 (441)	4.53 (661)	1.20 (47.4)	1.37
1729 (3500)	3.12 (452)	4.68 (678)	1.84 (72.6)	2.11
1852 (3750)	3.19 (463)	4.79 (694)	1.76 (69.3)	2.01
1976 (4000)	3.26 (473)	4.89 (709)	2.53 (99.8)	2.89
2100 (4250)	3.32 (482)	4.99 (723)	3.68 (145)	4.21
2223 (4500)	3.39 (492)	5.08 (737)	4.01 (158)	4.59
2346 (4750)	3.45 (500)	5.18 (751)	5.53 (218)	6.33
2470 (5000)	3.51 (509)	5.27 (764)	4.62 (182)	5.29

[a]Typical data scatter range ±5 percent.

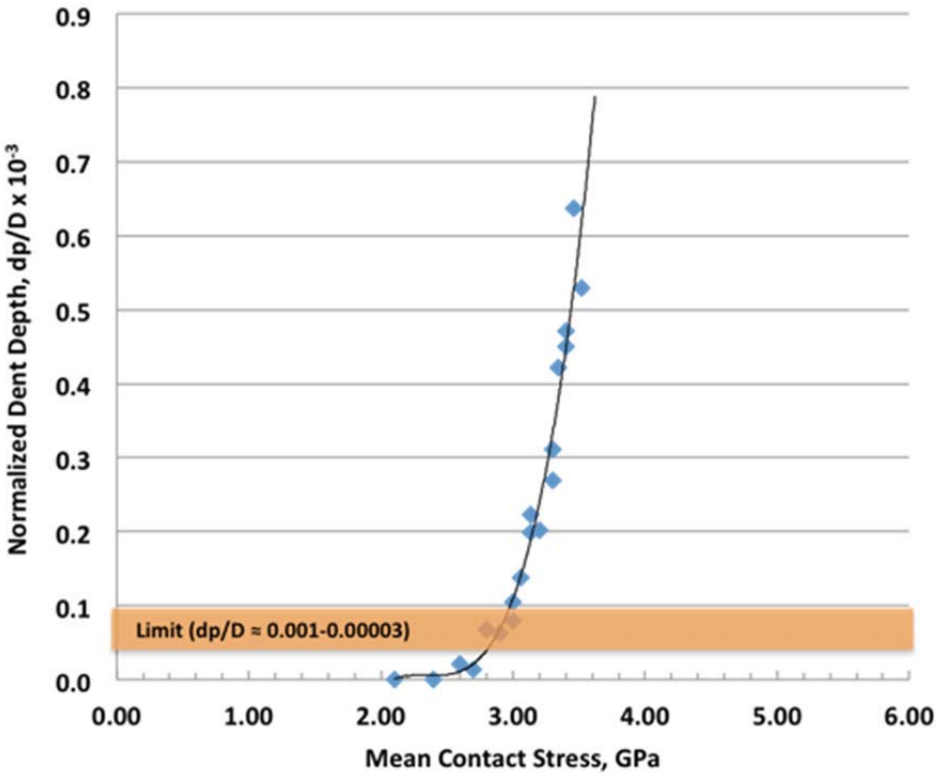

Figure 7. Normalized Dent Depth Versus Mean Hertz Contact Stress for Inner Race of a 50 mm 60NiTi Bearing Loaded by a Si_3N_4 Indenter Ball (8.74 mm dia.).

Notional Design Test Case

Spacecraft often use reaction wheel assemblies (RWA) for motion control functions. These assemblies consist of an electric motor driven heavy wheel supported on ball bearings. RWA's are typically hard mounted to a spacecraft structure in order to impart stabilizing forces and moments through inertial phenomena. A more complex device, the control moment gyroscope (CMG), employs multiple spinning wheels housed in one degree of freedom swivel mounts (gimbals) and can provide stabilization as well as pointing forces to the spacecraft. Both of these devices work in conjunction to traditional thrusters (chemical propulsion devices) to accurately position a spacecraft. To function properly, the bearings must provide low and stable running torque for the entire mission life that can span a decade or more. Despite modest operation loads and speeds, long-life is assured only if the bearings are lubricated properly and survive the rigors of launch without damage.

While spinning in orbit, bearing loads are low but during launch while the wheels are stationary the vibration and acceleration load environment can be severe. It is during this period of high load that bearing balls can dent bearing races affecting the long-term life and smooth operation of the device. The contact between the balls and inner race surface are particularly vulnerable due to geometrical effects. The ball-inner race contact areas are very small because of the race curvature and this leads to high stresses even at modest bearing load.

Estimating launch loads and designing robust yet lightweight mechanical systems capable of withstanding these loads can be as much an art as a science. Each rocket launch vehicle has its own unique vibration signature and, depending upon the payload configuration and isolation techniques used, random and steady acceleration loads transmitted to a particular payload can vary widely. These uncertainties often lead to the requirement that both analytical and experimental methods be used to verify that a device, such as a reaction wheel, can withstand anticipated load levels before being approved for flight.

The use of superelastic 60NiTi in reaction wheel bearing applications offers the potential for increased static load margins. To determine the potential magnitude of these improvements, a small rotor (5 kg) supported by two duplex pairs of small (R4 size) deep groove bore ball bearings is considered. Maximum contact stress limits for 60NiTi, 440C and the high carbide content REX20 tool steel are applied to the ball-inner race contact to estimate the maximum allowable g-forces the assembly can withstand. By comparing these resulting maximum load values, the benefits of using superelastic materials for races, and balls in wheel bearings can be determined.

A commercially available reaction wheel assembly shown in Figure 8 is the basis for the load modeling (Ref. 11). R4 ball bearing design and internal geometry is based upon catalogue values and are typical for such bearings (Ref. 12).

For simplicity, the rotor is modeled as being axially and radially symmetric. Bearing preload is neglected and the load case considered is a radial load passing through the center of mass equally counteracted by all four bearings. This calculation does not require a priori knowledge of the wheel geometry or inertia properties and thus can be undertaken without revealing any manufacturer's proprietary information. Radial bearing load capacity is lower than thrust load capacity because less than half the rolling elements support the load whereas for thrust load support all the ball-race contacts share the load equally. Examination of the radial load capability of bearings made with varying materials helps to clearly reveal the potential of using superelastic bearing materials.

Determining a specific launch load value is difficult. Developing a more generalized range of expected maximum loads is fairly straightforward. NASA provides a standard (GSFC-STD-7000) in which the maximum expected random vibration levels for payload components of various sizes (mass) are given (Ref. 1). By adding the random level to the steady acceleration g-forces one can establish a reasonable load level to impose when making the bearing load calculation. For payload components with masses less than 22.7 kg, the random load levels are 14.1 G_{rms} for qualification and 10.0 G_{rms} for acceptance. Typical steady acceleration forces for rocket launch are 1 to 3 g's. Thus for the RWA example being considered, a 5 kg wheel, the maximum applied rotor load is 17.1 g's (14.1 + 3).

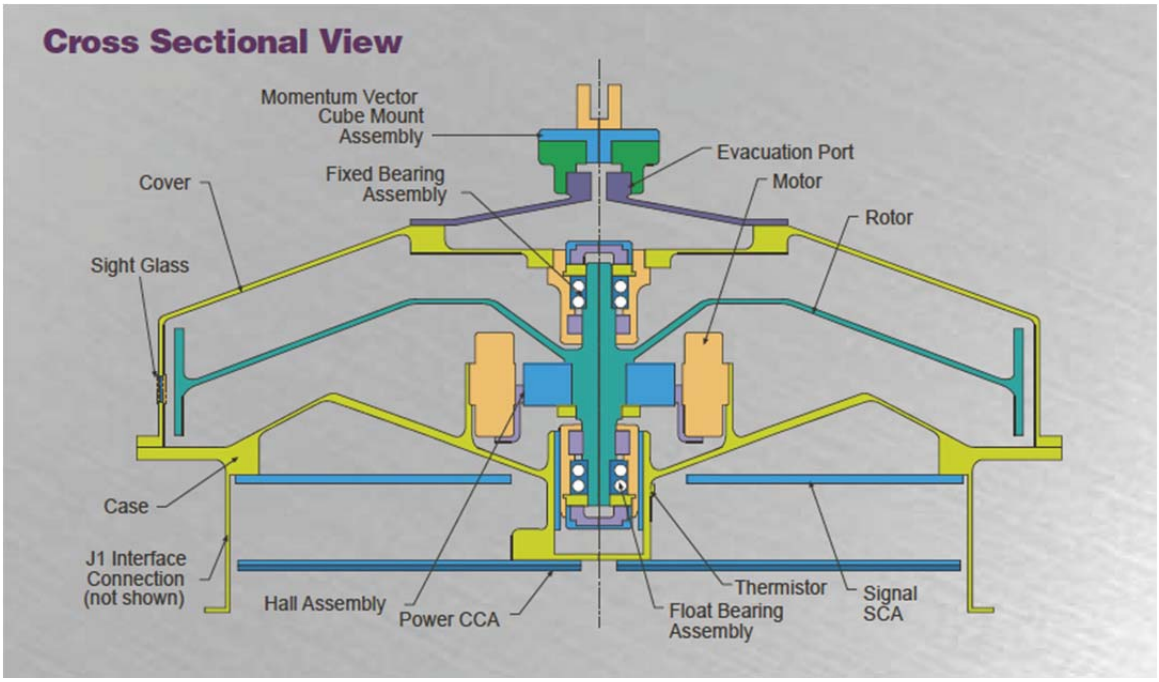

Figure 8. Typical Reaction Wheel Assembly. Figure Based Upon Honeywell Corporation Model HR 0610 Design (Ref. 11). 5 kg Wheel Supported on Four R4 Ball Bearings With Standard (Catalogue Values) Design (Ref. 12).

Table 3. Reaction Wheel Assembly Bearing Configurations Assessed

[Ball: 8.74 mm dia., Inner Race Curvature Radii: ball-path, 4.25 mm; cross-race, 1.27 mm.]

Configuration no.	Ball material	Race material	Limiting contact Stress,[a] GPa (ksi)	Single ball-race load limit, N (lb)
I	440C	440C	2.5 (350)	196 (44)
II	Si_3N_4	440C	2.5 (350)	138 (31)
III	60NiTi	440C	2.5 (350)	463 (104)
IV	60NiTi	60NiTi	2.5 (350)	846 (190)
V	Si_3N_4	60NiTi	2.5 (350)	374 (84)
VI	60NiTi	60NiTi	3.1 (450)	1780 (400)[c]
VII	Si_3N_4	60NiTi	3.1 (450)	801 (180)
VIII	[b]REX20	REX20	3.8 (550)	587 (132)
IX	Si_3N_4	REX20	3.8 (550)	467 (105)

[a]Mean Hertz contact stress.
[b]REX20 properties: Young's Modulus (E): 234 GPa; Poisson's Ratio (ν): 0.30.
[c]Hertz calculations may be invalid due to excessively deformed geometry.

Table 3 shows the bearing material configurations considered along with the bearing geometry assumptions and other pertinent details needed for the calculations.

The load capacity of the RWA bearing utilizing one of the configurations shown in Table 3 is determined by combining Hertz stress calculations with generally accepted bearing design relations that correlate ball-race contact stress to radial load capacity. For the Hertz calculations an automated spreadsheet is used in which the contact material properties, geometry and single ball-race load is input. The spreadsheet provides the mean and peak stress along with the contact area using the stress approximation equations developed by Antoine et al. (Ref. 13). The last column in Table 3 gives the single ball-race static load capacity for the nine materials and stress limit configurations considered.

To relate the single ball-race load capacity to radial load capacity of the R4 bearing, the relationships presented by Derner and Pfaffenberger and shown below are employed (Ref. 14):

$$F_R = 9Q_{max}/5 \quad (1)$$

In Equation (1), F_R is the bearing load capacity and Q_{max} is the single ball load capacity. The R4 bearing radial load capacity is then multiplied by four to account for the use of two duplex pairs of bearings in the RWA to get the overall wheel load capacity. This value is compared to the launch forces on the wheel to determine launch design margins for the various configurations. The calculation results are shown in Table 4.

Table 4. Reaction Wheel Launch Load Capacity

[5 kg wheel mass supported on two duplex pairs of R4 bearings.]

Configuration no.	Ball material	Race material	Shaft load capacity, kN (lb)	RWA load capacity, g
I	440C	440C	1.4 (316)	28.6
II	Si_3N_4	440C	1.0 (223)	20.2
III	60NiTi	440C	3.3 (748)	67.9
IV	60NiTi	60NiTi	6.1 (1368)	124.4
V	Si_3N_4	60NiTi	2.7 (604)	54.8
VI	60NiTi	60NiTi	[a]12.8 (2880)	[a]261.2
VII	Si_3N_4	60NiTi	5.8 (1296)	118
VIII	REX20	REX20	4.2 (950)	86.2
IX	Si_3N_4	REX20	3.4 (756)	68.5

[a]Load beyond yield strength of RWA shaft.

The load capacity results reveal some interesting insights. The two conventional bearing configurations (I-440C/440C and II-Si_3N_4/440C) have load capacity values near the g force requirements for rocket launch with additional margin to accommodate bearing preload and other forces neglected in the present simplified analyses. Another insight is that the use of a high performance material like REX20 offers a significant improvement in the load capacity, about 3-fold over the 440C bearing. It is this very improvement that drove the development of such high-carbide tool steels for heavy reaction wheels despite the poor corrosion resistance and higher production costs of REX20 (Ref. 15).

Finally, the estimated shaft load capacity for the all superelastic bearing configuration (VI) shows a value well beyond the bending load capability of an RWA wheel shaft sized for the bore of R4 bearings. This revelation suggests that in such an application, a superelastic bearing is essentially shockproof in that the bearing capability is beyond any load the rest of the instrument could withstand. Of course, designing a space mechanism with load capacity far in excess of requirements is unrealistic. Excess launch load capacity margins do not enhance system performance. However, the availability of more robust bearing materials, like 60NiTi may enable the use of fewer and smaller bearings thus reducing weight, power consumption and potentially cost. In addition, the enhanced corrosion resistance and non-magnetic properties of the NiTi alloys could enable mechanism designs with new capabilities.

Summary Remarks

This investigation confirms that bearings made with low modulus, hard and superelastic 60NiTi material exhibits extraordinarily high static load capacity. Indentation experiments using the inner race of a 50 mm bore ball bearing contacting a ceramic ball can withstand about 3 GPa mean stress before dents deeper than accepted limits are reached. This limiting stress value is consistent with the results obtained previously using flat plate 60NiTi specimens with indentation balls of varying diameters. The good agreement of the load capacity data collected under differing contact geometry configurations indicate that the Hertz stress relations can be used with confidence when designing bearings with respect to static load capacity.

Using a conservative stress limit of 3.1 GPa, the launch load tolerance of a small notional Reaction Wheel Assembly (RWA) supported on R4 sized bearings utilizing different materials was evaluated. The results show that the baseline RWA supported by 440C steel bearings can withstand launch vibration levels of about 25 g's. The use of the super-hard tool steel REX20 increases the launch load tolerance by a factor of three or more albeit while introducing bearing corrosion concerns. The use of 60NiTi provides an order of magnitude more load tolerance than the baseline 440C steel bearing case while imparting improved corrosion protection.

The enhanced load capacity enabled by the use of superelastic bearing materials like 60NiTi offer the opportunity to utilize smaller and fewer support bearings with commensurately lower operating friction. In future systems that may require larger wheels, the ability to withstand higher static loads may be an even stronger design driver for the continued development of superelastic bearings.

Acknowledgements

The authors wish to acknowledge NASA's ISS Project Office and the NASA Engineering and Safety Center for their support of this work. The authors also acknowledge the technical contributions made to this work by NASA Glenn Research Center's Nathan Wilmoth, Walter Wozniak, and Fransua Thomas and also the valuable race dent measurements made by Justin Rowe of the Oregon State University during his internship at NASA Marshall Space Flight Center (MSFC). Without their assistance in specimen preparation and testing have enabled this work.

References

1. General Environmental Verification Standard-Goddard Space Flight Center Standard-STD-7000, NASA GSFC, Greenbelt, MD, April 2005.
2. A.R. Leveille and J.J. Murphy, "Determination of the Influence of Static Loads on the Output Torque of Instrument Ball Bearings," in Proceedings of the Charles Stark Draper Lab. International Ball Bearings Symposium, (1973).
3. D.W. Smith, A.R. Leveille, M.R. Hilton, and P.C. Ward: "REX 20/Si_3N_4 Control Moment Gyroscope Bearing Development," Proceedings of the 32nd Aerospace Mechanisms Symposium, May 13-15, 1998, Cocoa Beach, FL, NASA CP-1998-207191, pp. 223-235, 1998.
4. C. DellaCorte, S.V. Pepper, R. Noebe, D.R. Hull, and G. Glennon, 2009, "Intermetallic Nickel-Titanium Alloys for Oil-Lubricated Bearing Applications," NASA/TM—2009-215646.
5. C. DellaCorte, R. Noebe, M.K. Stanford, and S.A. Padula, "Resilient and Corrosion-Proof Rolling Element Bearings Made From Superelastic Ni-Ti Alloys for Aerospace Mechanism Applications," Proceedings of the 2011 ASTM Rolling Element Bearings Conference, Anaheim, California, April 13-15th, 2011 and NASA/TM—2011-217105.
6. C. DellaCorte, L.E. Moore, III, and J.C. Clifton: "Static Indentation Load Capacity of the Superelastic NiTi for Rolling Element Bearings," NASA/TM—2012-216016, May 2012.
7. C. DellaCorte, L.E. Moore, III, and J.C. Clifton: "The Effects of Pre-Stress on the Static Indentation Load Capacity of the Superelastic NiTi," NASA/TM—2012-216479, January 2013.
8. C. DellaCorte, L.E. Moore, III, and J.C. Clifton: "The Effects of Indenter Ball Radius on the Static Load Capacity of the Superelastic 60NiTi for Rolling Element Bearings," NASA/TM—2014-216627, 2014. To be published.
9. C. DellaCorte and W.A. Wozniak: "Design and Manufacturing Considerations for Shockproof and Corrosion-Immune Superelastic Nickel-Titanium Bearings for a Space Station Application," NASA/TM—2012-216015 and Presented at the 41st Aerospace Mechanisms Symposium, Pasadena, CA, May 2012.
10. B.J. Hamrock, S.R. Schmid and B.O. Jacobson: Fundamentals of Fluid Film Lubrication, 2nd Edition, Chapter 21, Marcel-Dekker, 2004, NY.

11. Data Sheet: Honeywell Model HR 0610 Reaction Wheel, Document #DFOISR:03-S-1924, December 2003, Honeywell Corporation, Phoenix, AZ.
12. Barden Super Precision Ball Bearings Catalogue, D/SPC/1/USA/113/T, Danbury, CT, 2013.
13. J.F. Antoine, G. Abba, C. Visa, and C. Sauvey: "Approximate Analytical Model for Hertzian Elliptical Contact Problems," ASME Journal of Tribology, volume 128, issue 3, pp. 660-664, March 2006.
14. W.J. Derner, and E.E. Pfaffenberger: "Rolling Element Bearings," in CRC Handbook of Lubrication: Theory and Practice of Tribology-volume II-Theory & Design, edited by E.R. Booser, pp. 495-537, 1983.
15. W. Park, M.R. Hilton, P.C. Ward, G.W. Henderson, A. R. Leveille, D.E. McClintock, and D.W. Smith, "Microstructure, Fatigue Life and Load Capacity of PM Tool Steel REX20 for bearing Applications," Lubrication Engineering, volume 55, number 6, pp. 20-30, 1999.